NASA TECHNICAL MEMORANDUM

NASA TM X-73379

(NASA-TM-X-73379) THE APPLICATION OF DIGITAL TECHNIQUES TO THE ANALYSIS OF METALLURGICAL EXPERIMENTS (NASA) 45 p HC A03/MF A01 CSCL 11F G3/26

N77-23239

Unclas 29060

THE APPLICATION OF DIGITAL TECHNIQUES TO THE ANALYSIS OF METALLURGICAL EXPERIMENTS

By Thomas J. Rathz
Space Sciences Laboratory

February 1977

NASA

George C. Marshall Space Flight Center
Marshall Space Flight Center, Alabama

TECHNICAL REPORT STANDARD TITLE PAGE

1. REPORT NO.	2. GOVERNMENT ACCESSION NO.	3. RECIPIENT'S CATALOG NO.
NASA TM X-73379		

4. TITLE AND SUBTITLE

The Application of Digital Techniques to the Analysis of Metallurgical Experiments

5. REPORT DATE

February 1977

6. PERFORMING ORGANIZATION CODE

7. AUTHOR(S)

Thomas J. Rathz

8. PERFORMING ORGANIZATION REPORT #

9. PERFORMING ORGANIZATION NAME AND ADDRESS

George C. Marshall Space Flight Center
Marshall Space Flight Center, Alabama 35812

10. WORK UNIT NO.

11. CONTRACT OR GRANT NO.

13. TYPE OF REPORT & PERIOD COVERED

Technical Memorandum

12. SPONSORING AGENCY NAME AND ADDRESS

National Aeronautics and Space Administration
Washington, D.C. 20546

14. SPONSORING AGENCY CODE

15. SUPPLEMENTARY NOTES

Prepared by Space Sciences Laboratory, Science and Engineering

16. ABSTRACT

The application of a specific digital computer system (known as the Image Data Processing System) to the analysis of three NASA-sponsored metallurgical experiments is discussed in some detail. Some of the basic hardware and software components of the Image Data Processing System are presented as deemed necessary for the understanding of the text. Many figures are presented in the discussion of each experimental analysis in an attempt to show the accuracy and speed that the Image Data Processing System affords in analyzing photographic images dealing with metallurgy, and in particular with material processing.

ORIGINAL CONTAINS
COLOR ILLUSTRATIONS

17. KEY WORDS

18. DISTRIBUTION STATEMENT

Unclassified — Unlimited

Thomas J. Rathz

19. SECURITY CLASSIF. (of this report)	20. SECURITY CLASSIF. (of this page)	21. NO. OF PAGES	22. PRICE
Unclassified	Unclassified	47	NTIS

TABLE OF CONTENTS

LIST OF ILLUSTRATIONS

LIST OF ILLUSTRATIONS (Concluded)

LIST OF TABLES

THE APPLICATION OF DIGITAL TECHNIQUES TO THE ANALYSIS OF METALLURGICAL EXPERIMENTS

I. INTRODUCTION

The extraction of information from radiographic and photographic films [1,2] is a task with which many disciplinary fields have been concerned for some time [3], especially within the fields of astronomy [4-6], medicine [7,8], and metallurgy [9-13]. With the advent of high-speed computers and present-day microdensitometers, cataloging, analyzing, and interpreting data from film images have been greatly simplified and extended.

Inherent within any system whose purpose is to process images by digital techniques are factors that must be considered before determining whether a system of this type will be beneficial for extracting the desired data from film images. Some factors used for arguing in favor of digital methods are the excellent quality and quantity of data obtained by computer processing of images via such techniques as contrast variation, geometric manipulation, multipictorial analysis, Fourier transformation techniques, etc. [3,7,14]. These factors must be weighed against the possible disadvantages of digital methods such as computer time requirements, limited computer core, the applicability of the available programs to a specific image analysis, or poor resolution of film images due to microdensitometer limitations (i.e., scanning time versus signal-to-noise and image distortion due to aperture size). Most arguments for or against digital analysis of images ultimately depend upon the system (hardware) being used and not necessarily upon the techniques (software) available within this system [5,15,16]. If necessary, the operator can formulate his own computer programs to satisfy his requirements. Even some of the hardware problems such as image distortion due to different aperture sizes can be reduced by the application of specialized programs (Fourier transformations coupled with suitable filters). Ideally, then, the only limitations to using digital computers for image analysis are those imposed by the system hardware necessary to analyze an image and not those factors concerning the quality of the information contained within a digitized image.

Many investigations have been performed to determine the feasibility of using digital techniques for the study of radiographic materials and for microstructural material analysis. The microstructural evaluation by image analysis is a discipline that has already received many years of investigation via the use of such specialized machines as IMANCO's Quantimet 720 series or Zeiss's Micro-Videomat series, which usually employ Vidicon or Plumbicon camera tube scanners rather than a microdensitometer type scanner [12,13]. The radiographic material analysis is similarly well documented, but much of the image enhancement done in this area has had the enhancement itself as the experiment [9-11]. The intent of this report is to present a general discussion of the use of a specific image enhancement system, the Image Data Processing System (IDAPS), as applied to the analysis of several metallurgical experiments characterized in one way by radiographic and microstructural analysis techniques.

A discussion of the detailed results obtained from this computer system will be presented so that the merit of using such a tool for this type of experimental analysis can be inferred. This report will describe the essentials of the experiments being analyzed, but it will not go into depth concerning the results or conclusions of each experiment (these can be found in the specified references).

II. COMPUTER FACILITIES

IDAPS, which is capable of performing a wide variety of image manipulations, is available at Marshall Space Flight Center. The system, shown schematically in Figure 1a and pictorially in Figure 1b, was designed for the analysis of Skylab/ATM S-056 X-Ray Telescope experiment data [4]. Table 1 lists many of the programs available to the user from the IBM-360 host computer (not shown in Fig. 1b). Interfaced with the host computer is the terminal minicomputer (located to the left in Fig. 1b) which has its own programs (Table 2) that are immediately available upon the operator's request.

The master monitor (located in back of the keyboard in Fig. 1b) allows the user to have control over all functions of IDAPS. The master monitor displays a listing or "menu" of very general operations from which the user selects the one that he wishes to be performed. The monitor will then display a submenu listing specific programs (Table 1) available within the selected operation, or it will give a list of the possible settings on peripheral equipment that will be used. If the operator is choosing a particular program and not equipment settings, then the master monitor displays still another list containing the program parameters.

Inputting an image from photographic medium is done via the scanning microdensitometer, which is the center piece of equipment in Figure 1b. Scanning speeds, aperture size, and film illumination as well as data output are controlled also from the master monitor. The digitized data obtained from the microdensitometer, consisting of an N × N array of gray scale values (GSV) each of which ranges from 0 (black) to 256 (white), correspond to the localized transmittance at specific locations of the film image. The matrix size depends on the film image size and may be as large as 2048 × 2048; but, because of limited monitor dimensions, only 480 × 480 sized portions of the original array can be displayed at any one time. Once the image is scanned and digitized, it can be stored on (a) magnetic tape for future input, (b) the minicomputer disk for immediate presentation on one of two black and white monitors, or (c) filed within the IBM-360 for manipulation purposes.

When image inputting is complete, analysis can then begin by selecting one or more of the programs from the master menu. Only a few of these programs which are pertinent to this report will be explained in detail. (A complete description can be found in References 14 and 17 which also describe the IDAPS hardware components more comprehensively.)

There are three important operations that are available from the minicomputer and are summoned directly from the master monitor keyboard and not from a menu. These are the coordinate, histogram, and slice operations. They are explained in Table 2, and their importance lies in their immediate availability and in their ability to quickly extract and display quantitative information from images.

Some of the IDAPS operators available through the IBM-360 (Table 1) are listed here in detail so that there will be a clear understanding of what each program does when it is referred to later in this report:

a. Automatic scale — Linear/nonlinear GSV adjustment. Performed directly to original image to enhance contrast by expanding, contracting, or deleting certain GSV ranges.

b. Extract subframe — A portion of the original image can be obtained and displayed as a completely separate image.

c. Insert — A portion of one image (the overlay) may be inserted into another image (the underlay). The user may specify where the overlay is to be inserted in the underlay.

d. Frame — The input image is completely surrounded by a display mask. This mask can contain annotations, a histogram of the entire input image, and a grid overlayed on the image.

e. H-D correction — Quantitative data from film images require knowledge as to how the desired parameter (i.e., solar temperature, material concentrations, etc.) varies with GSV. This requires the use of a calibration curve which will also give the correction needed for the nonlinear response of the film. The calibration curve is presented by this program in the form of a listing of the pertinent parameter versus GSV.

f. Isogram — Contours of constant GSV are found, marked, and displayed according to user discretion.

g. Magnify — This program allows expansion or reduction of an image by any fractional factor. Expanded image is limited in size to a 2048 × 2048 array.

h. Alter — This program allows the user to transform the original image GSV into an image or matrix of GSV corresponding to the desired parameter as specified by a calibration curve or corresponding to the operator's own requirements.

i. Pseudocolor — Each GSV or group of GSV's of an image can be assigned a specific color for enhancement of areas having minute contrast or for selective emphasis of particular areas on the image.

Although not deemed necessary in any of the preceding experimental analyses, the fast Fourier transform is one of the more powerful programs, together with its associated filters (convolution, high/low pass, etc.), that can be found in IDAPS. When transforming/filtering is performed, unwanted optical system effects present within an image such as defocus, spherical aberrations, intervening atmospheric degradation, geometric distortion, etc., can be reduced to some extent [1,7]. Some understanding of Fourier optics is necessary for an operator to reasonably and effectively apply the preceding program.

As soon as analysis of an image has been performed, the data can be retrieved in several ways: (a) by placing the enhanced image on film via the film recorder, (b) by "dumping" the data on magnetic tape, (c) by printing the data in numerical form, or (d) by copying the image from one of the monitors via a low resolution video facsimile machine. The method used to retrieve the data ultimately depends upon the user's discretion as to which form of output will present in the most informative way the results of the analysis performed on IDAPS.

III. APPLICATIONS

The discussion of the metallurgical applications of IDAPS is centered around three NASA-sponsored experiments dealing with the processing of materials in a microgravity environment. These experiments are: (a) Study of Mixing between Liquid Metals [Space Processing Applications Rocket (SPAR) Experiment No. 74-18/1], (b) Study of Surface Tension Effects on Liquid Metals [Apollo-Soyuz Test (ASTP) Experiment MA-041], and (c) Homogenization Experiment of Metal Alloys (ASTP Experiment MA-044). The nature of the results of each experiment made it desirable to obtain part of the analysis from images on photographic medium to minimize destructive-type evaluation. The same basic information was needed for each experiment: the location and the quantity of one material within a dissimilar material. The IDAPS is shown to be a very effective tool in fulfilling these two requirements.

A. Study of Mixing Between Liquid Metals

One particular application of the IDAPS system concerned the characterization of an experiment dealing with the stability and buoyancy effects in near-zero gravity of two different liquid metals initially coupled together as shown in Figure 2. Three of these bimetal systems aligned orthogonally to each other were melted and resolidified during the 5 min of low gravity provided by the first SPAR [18, 19].

By using X-radiography on the returned flight samples, the flow that had taken place between the metals could be seen readily, thus giving some idea of the residual gravitational force present as well as the critical force necessary to initiate flow. This flow visualization was possible because the bimetal system (indium and indium — 20 wt. % lead alloy) had X-ray absorption coefficients whose difference gave enough contrast on the film to allow simultaneous radiographs of both metals. Once radiographs of each entire sample were made at many degrees of rotation to the incident X-ray beam, 2 mm thick slices were taken perpendicular to the sample's longitudinal axis. These slices, when laid flat, were X-rayed also to see how the internal flow compared to the flow as viewed from the overall radiographs.

The contrast between the two materials on the film was visually quite evident; but when displayed on IDAPS, much more detail clearly could be seen. The image of one slice of sample No. 6 is shown in Figure 3a[1] to which the linear automatic-scale program was applied, resulting in edge enhancement and in a slight increase in contrast.[2] Figure 4a shows what an original image looked like before any image manipulation. The linear automatic-scale program could not be used on these entire sample images as used in Figure 3a because the GSV's of the indium material were darker than the GSV's surrounding the indium-lead alloy; thus, when attempting to edge enhance the indium-lead material by "blackening out" the surrounding GSV's, the indium material would also be "blackened out." This problem was solved by using the alter and insert programs in combination: half of an original entire sample image could be edge enhanced and then this resultant image merged with the remaining half-image likewise edge enhanced. Two of the three flight samples whose images have been edge enhanced in this way are shown in Figures 4b and 5a.

To further enhance the location of the two metals, pseudocoloring was performed. Before executing this program, the histograms of GSV's (provided at the bottom of the figures by the frame program) were used to give some indication of which GSV's corresponded to each metal and to their approximate interface within each image. Figures 3b, 4c, and 5b are the pseudocolored

1. The frame surrounding the image was provided by IDAPS as described in Section II.

2. Keep in mind the loss of clarity that occurs when converting images to photographic medium as compared to an image displayed on a high resolution video screen.

representations of the originally scanned images of Figures 3a, 4b, and 5a, respectively. In these images the indium-lead material is colored red, the indium is blue, and the approximate interface is the narrow band of yellow-green-purple colors. Note that after pseudocoloring there can be seen in the center of Figure 5b an area that shows definite beginnings of fluid motion; this is an effect not readily seen in Figure 5a. The effect was similarly found in flight sample No. 2, not shown here. Because of X-ray edge effects and because these figures are not pseudocolorings of the edge enhanced images, there exists the false appearance that one metal is entirely enclosed within the other.

To obtain a more direct visualization of the flow that took place, the slice program of IDAPS was used which provides a plot of GSV's versus distance. An example taken from the low-resolution video facsimile copier is given in Figure 6; the white line in the image marks the location of the slice. Many of these programmatic slices were taken perpendicular to the longitudinal axis for each sample. Composites were then made of these plots for each sample at each of the several different degrees of rotation relative to the direction of the incident X-ray beam, thus giving a three-dimensional view of the flow that had taken place. An example is given in Figure 7 of sample No. 6 rotated zero degree to the incident X-ray beam.

One of the unique advantages of IDAPS is the ability of a user to write his own program for extracting particular information from an image. Such was the case for analyzing this experiment because determining the extent of flow between the indium and indium-lead alloy demanded the finding of an interface between the two materials. The interface could be found by determining the greatest change in GSV for a unit fixed length on each line of image data. Once found, the interface would be marked by a white line so as to be clearly evident. Limited success has been attained with such a program at present; modifications are being made for including a line-fitting procedure which will eventually produce a smooth interface curve and data on the accuracy of the fit.

B. Study of Surface Tension Effects on Liquid Metals in Microgravity

On ASTP an experiment was performed to detect surface tension convection that may be caused by a step-like compositional gradient between two dissimilar liquid metals [20,21]. The two materials (lead and lead – 0.05 at. % gold alloy) were initially coupled as shown in Figure 8. The experiment was performed in both wetting and nonwetting canisters, and each of these was at two different temperatures. The samples were left in the molten phase for 2 hours so that any convective stirring effects would clearly be evident; otherwise, the conventional diffusion profile would be present.

Autoradiography was the characterization scheme used for determining the gold concentration distribution within the samples. First, standards of known gold-lead composition and each flight sample, sliced in half longitudinally, were mounted together and neutron activated; then, each assembly was placed in contact with film which was sensitive to the energy of the beta-particles emitted from the decaying gold. The film images of the standards were scanned by IDAPS using the H-D correction program, which automatically provided a curve of gold-concentration versus GSV's obtained by straight-line interpolation between the points of the calibration data. This curve was then used (via the alter program) to change the GSV's of the originally scanned image into an image consisting of gold-concentration values; i.e., instead of seeing the image on a monitor as shades of light and dark areas that vary as film transmittance, the image was seen as varying shades of light and dark areas that corresponded to changing amounts of gold concentration (Fig. 9).

Once the original image had been converted to gold concentration values, many choices of characterization schemes existed with the use of IDAPS. One approach taken was that of pseudocoloring specific ranges of gold concentration as given in Table 3. Using this table of values for all specimens, one is immediately able to compare qualitatively the extent of diffusion and convection in each sample as shown in Figures 10 and 11. Figures 10a and 11a show the ground-based (GB) samples identically processed as were their respective space flight (SF) samples in Figures 10b and 11b.

Another technique employed was the use of the isogram program. This allowed quick determination of the extent of the gold distribution in ranges broader than those used for pseudocoloring. One example is shown in Figure 12 in which each contour represents that concentration of gold in atomic ppm as so labeled.

Images analyzed by the preceding two methods have good pictorial and semiquantitative value. To gather some definite quantitative data, the previously described slice program was used. This operation provided a plot of gold concentration versus distance which in turn yielded numerical data in the form of the graphs in Figure 13. Figure 13a represents the percent of total gold present in each of many slices, taken in the direction of the longitudinal axis of

Figure 9, as a function of the distance out from the central longitudinal slice; Figure 13b is one example of a plot of the percent of total gold present at each location in a slice as a function of the location in that slice. From such information, the overall gold distribution was detectable not only in the radial direction but also in the longitudinal direction.

The microstructure of the samples was investigated by using the magnification program on a particular area of the sample. Then, a suitable pseudocoloring scheme similar to that used in Table 3 was applied to the image, the results of which are shown in Figure 14. This permitted comparison of the grain structure as well as areas of gold accumulation between flight and ground samples.

C. Study of the Homogenization of Metal Alloys

An analysis similar, in part, to that performed in the surface tension effects experiment was used to quantitatively measure the microstructural homogeneity and stoichiometry of melted metals. An experiment was performed on ASTP to study the effects of the low-gravity environment on the melting and solidification of two material systems: aluminum — 50 at. % antimony and zinc — 20 at. % lead [22,23]. The materials were initially in the form depicted in Figure 15. Both composite metals were premelted within their uncapped graphite crucibles under an argon atmosphere.

At present, only the AlSb material has been investigated using the IDAPS facility. This was done by first obtaining photomicrographs of particular areas of the sliced and polished samples from both the low- and one-gravity [ground-based test (GBT)] processed materials (Fig. 16). The negatives of these photographs were converted into 35 mm slides which could then be scanned by IDAPS. When histograms were performed on the entire area of these images, information on the area fraction of the different phases of AlSb present in each sample was immediately available (Fig. 17). The accuracy of this information was checked by using a planimeter to measure the relative areas of each phase seen on the film. The two results agreed to within 2 percent, most of the difference being attributable to human limitations and inaccuracies in measuring with a planimeter the fine structure present on the film.

Using the data of Figure 17, pseudocoloring was performed in which colors were assigned to those GSV's that were indicative of each phase in the AlSb. The resultant picture (Fig. 18) not only enhanced the different phases but removed unwanted surface artifacts for clearer presentation of the microstructure and also verified the phase-to-peak correlation of Figure 17.

The histogram technique was performed several more times to gather additional quantitative data. This was done in two ways: First, microphotographs were taken completely across a section of both the low- and one-gravity samples; then, repeating the procedure used to obtain Figure 17 for each of these new images, quantitative microstructural data shown in Figure 19 were obtained for comparative characterization. Second, two of the photomicrographs were compared as shown in Figure 20 by using IDAPS to extract data as a function of picture area.

IV. CONCLUSION

For the three experimental analyses described, IDAPS proved to be a very quick and efficient tool for visually and quantitatively evaluating materials and for examining those factors that contribute to the overall processing of those materials. The possible merits of using a digital computer such as IDAPS for enhancing metallurgical images have been discussed in some detail, but only through the figures presented can an impression of IDAPS's abilities be conveyed. These abilities lie in the machine's diverse programs and the user's techniques in applying them, as well as the ease and speed of extracting data from film images.

The three experiments described used IDAPS for their analysis because this computer offered the necessary image manipulation functions to obtain the required results and because each experimental analysis needed photographic characterization which made IDAPS a most appropriate tool to utilize. For the purposes of this report, however, these experiments offered ideal situations for describing the uses of a digital computer for general metallurgical problems and analysis. These uses are summarized as follows:

a. Study of Flow Between Liquid Metals in Low Gravity — IDAPS gave clear, qualitative images of the flow within each sample and allowed ease of comparison between samples. Details not seen in the original image were made visible through pseudocoloring. Three-dimensional qualitative information was extracted, and three-dimensional quantitative data are a real possibility [10].

b. Study of Surface Tension on Liquid Metals in Microgravity — Quick and accurate quantitative information on microscopic processes occurring within a large surface image was obtained. The extent of diffusion between and within samples was easily observed and quantified, thus allowing an accurate description of the surface tension effects.

The use of a calibration curve for image conversion into units other than GSV's proved to be most fruitful in attaining the desired results for this type of analysis. When this can be done, many avenues are opened for extracting excellent information from the converted image (pseudocoloring, isogramming, slicing, histogramming, etc.)

c. Microstructural Study of AlSb — IDAPS offers accurate and immediate retrieval of quantitative information on the macroscopic processes occurring within a large surface image. The sample homogeneity, as determined by area fraction of different phases present in the material, could be found by simply using the histogram operator on part of or on an entire microphotograph image. Pseudocoloring of the photomicrographs gave improved contrast and eliminated unwanted surface artifacts. It should be noted that there are other specialized surface analysis machines (as noted in Section I) that are probably more efficient and perhaps more accurate than IDAPS in performing this type of analysis. Possible advantages of IDAPS over these other machines could include the increase in contrast between areas on an image, the ability to analyze images via operator-written programs, and the space available for storing images. Perhaps by combining the strong features of both types of machines, a better way of analyzing surface images of metals could be found.

The user, then, is limited to extracting data from an image only by his own inabilities to intertwine the computer operations and not by the nonavailability of programs. If need be, the user can develop his own programs. If an experimenter can obtain his data in photographic form, the power of a digital machine such as IDAPS cannot be overestimated for its speed, ease of handling, and information extractability in analyzing metallurgical experiments.

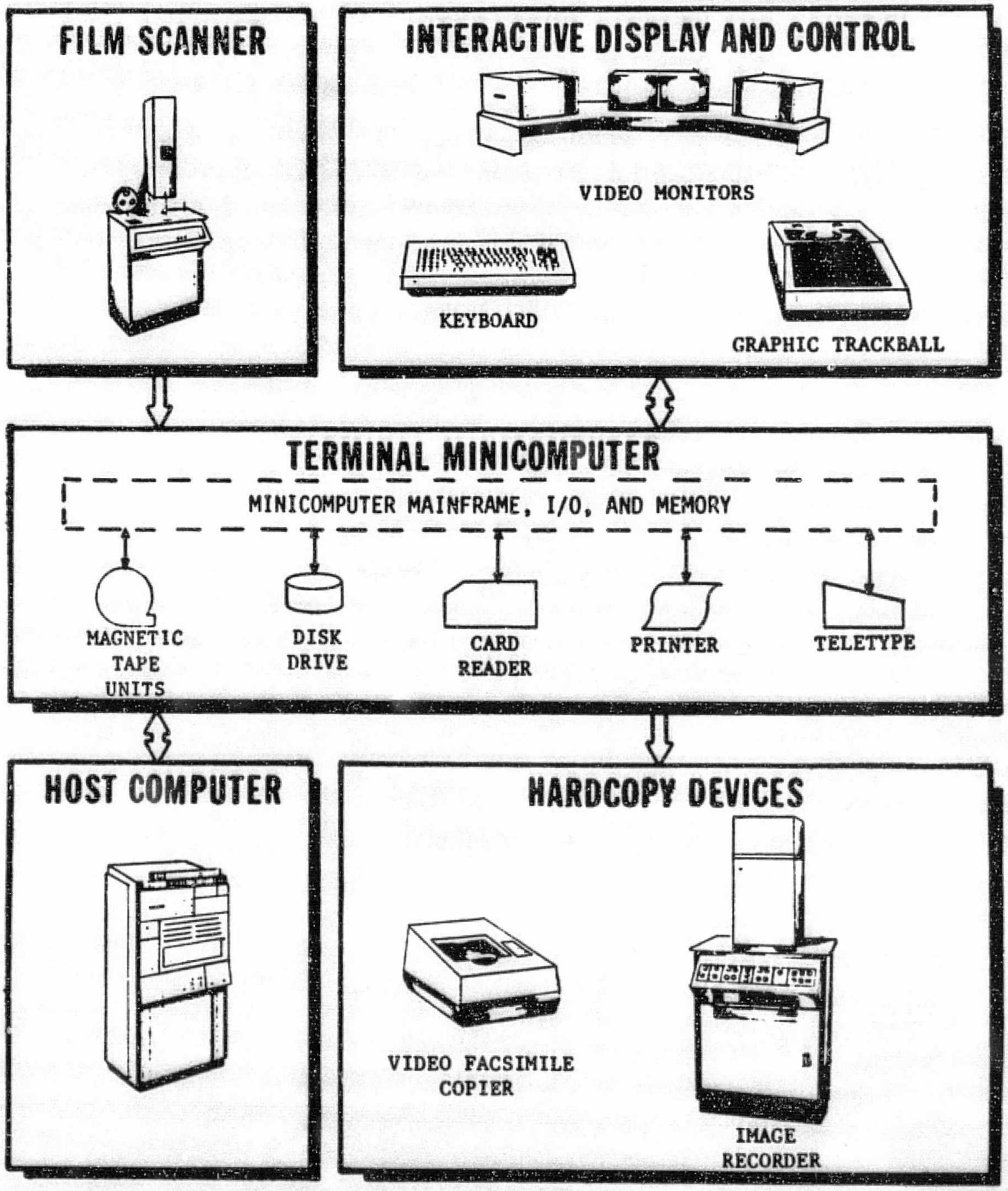

a. IDAPS schematic.

Figure 1. IDAPS: schematic and pictorial representation.

b. IDAPS facility; not shown is the IBM-360 host computer.

Figure 1. (Concluded).

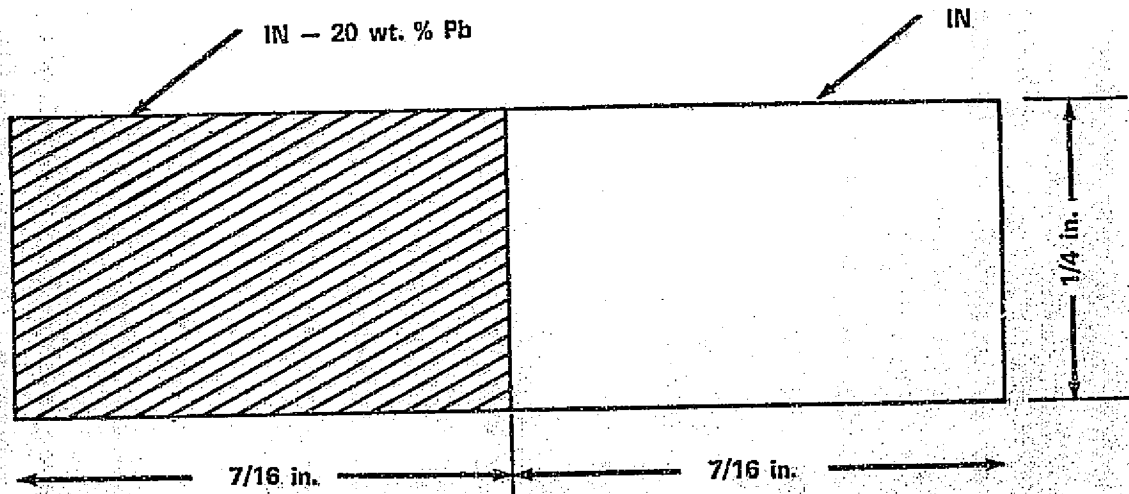

Figure 2. Cylindrical sample configuration for SPAR Experiment No. 74-18/1.

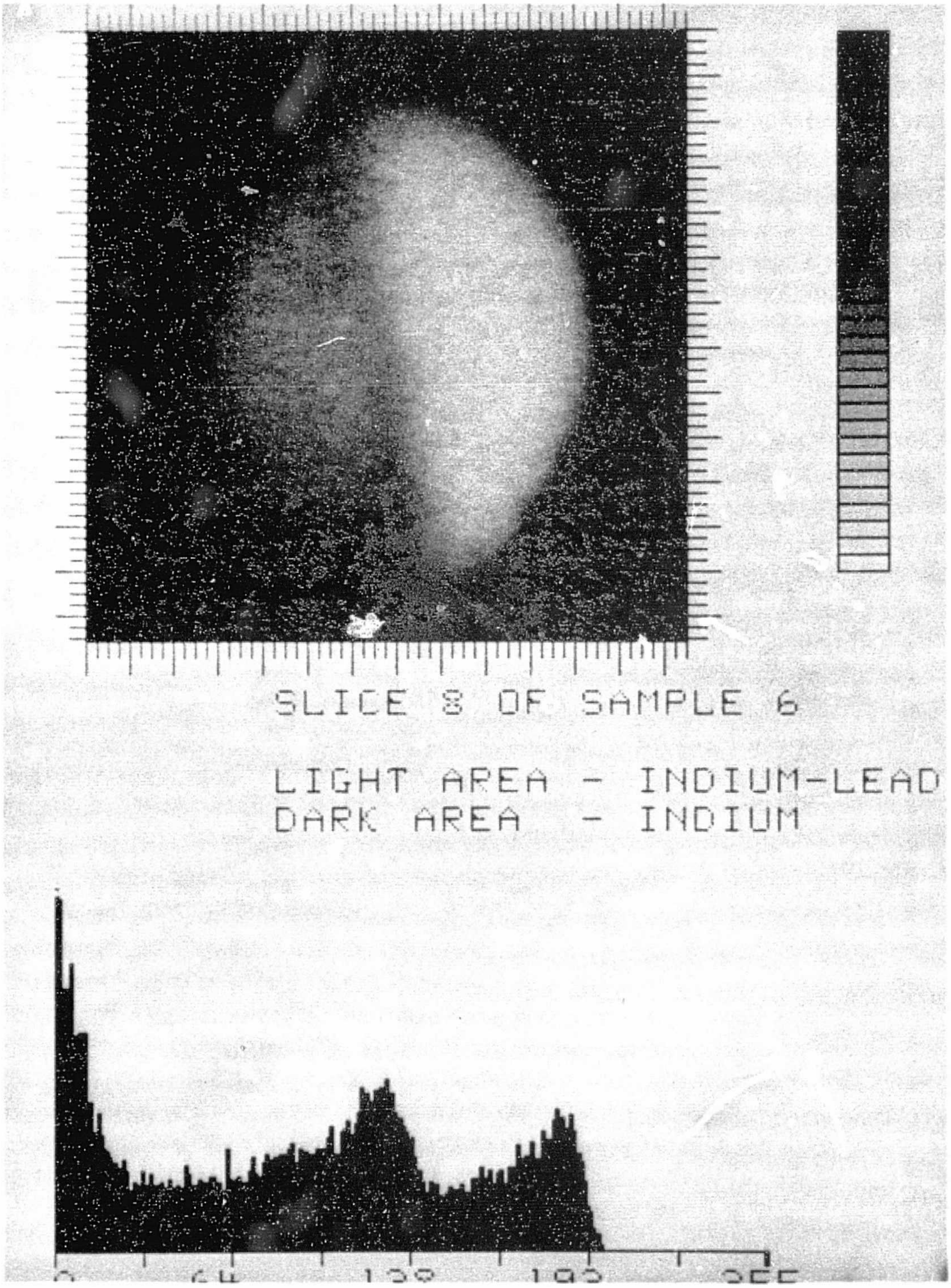

a. Edge and contrast enhanced.

Figure 3. Image of slice of sample No. 6.

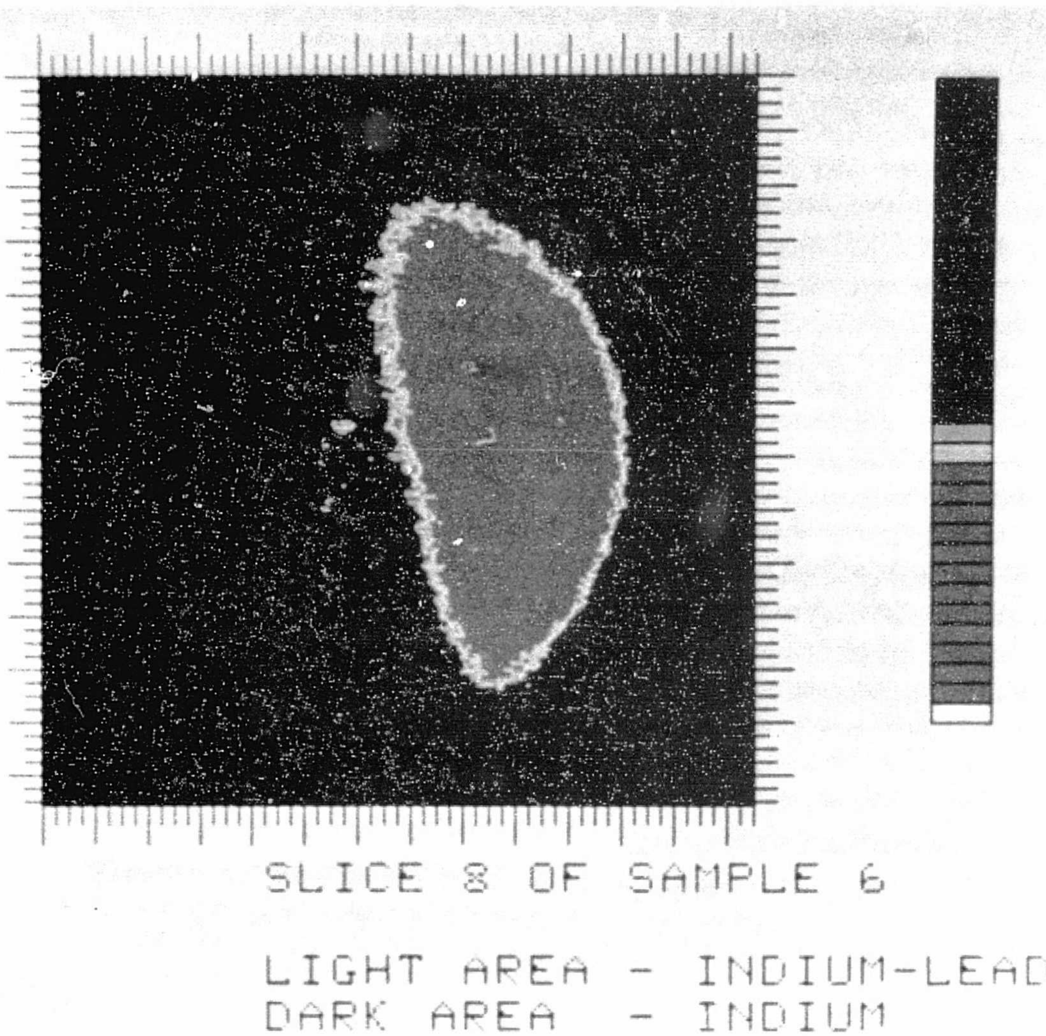

b. Pseudocolored: red area represents indium-lead alloy; blue, indium; yellow-green-purple, interface.

Figure 3. (Concluded).

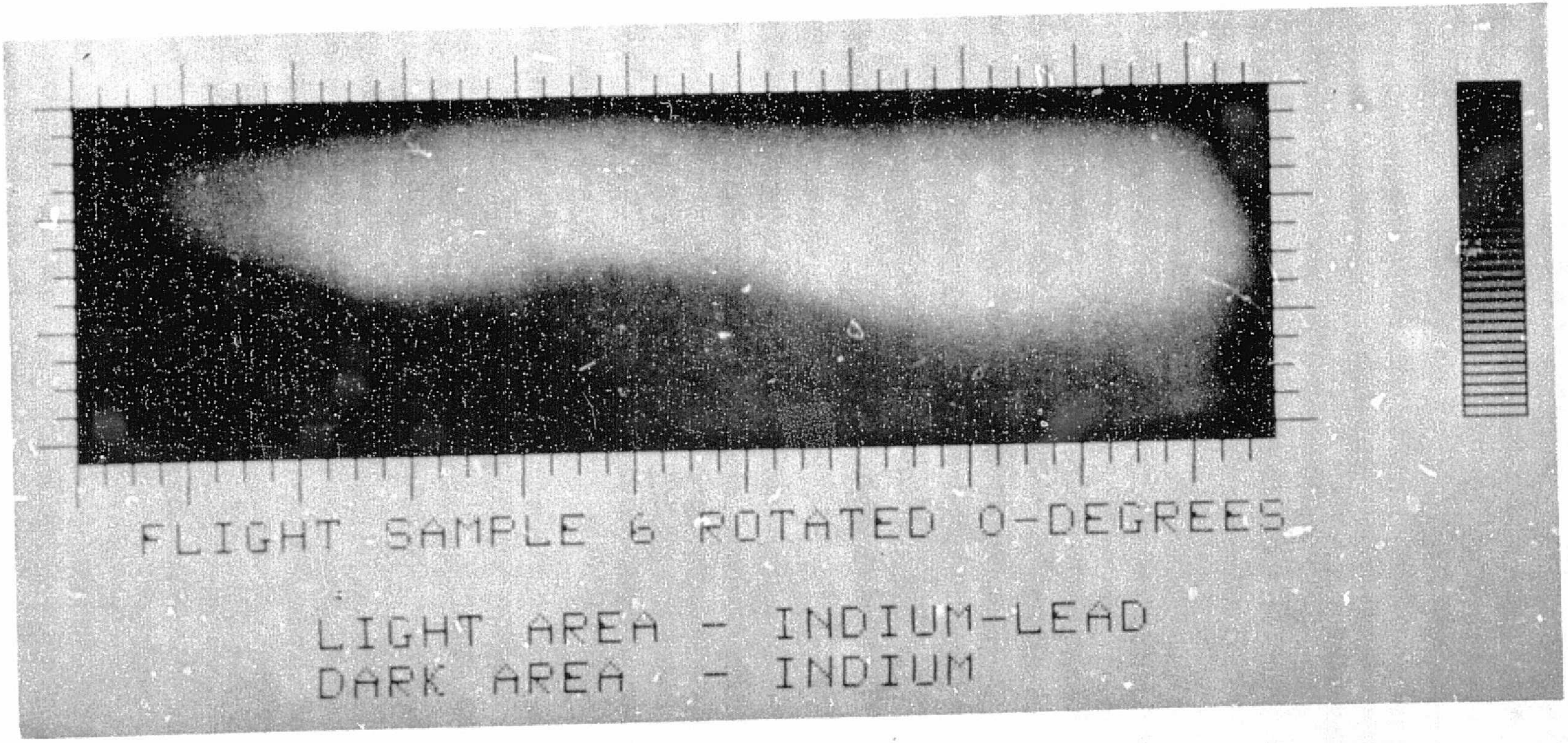

a. Originally scanned image.

Figure 4. Entire image of sample No. 6.

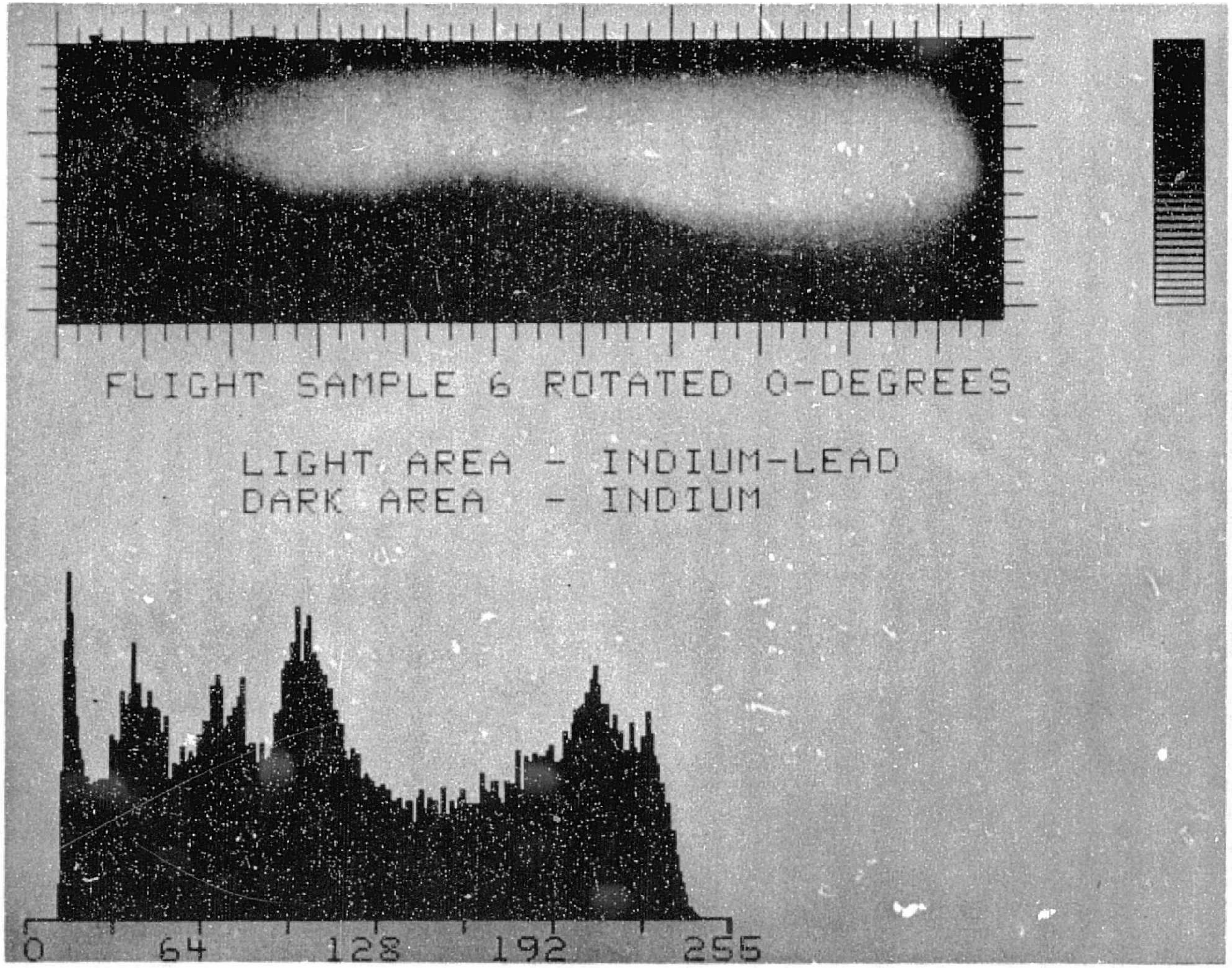

b. Edge enhanced.

Figure 4. (Continued).

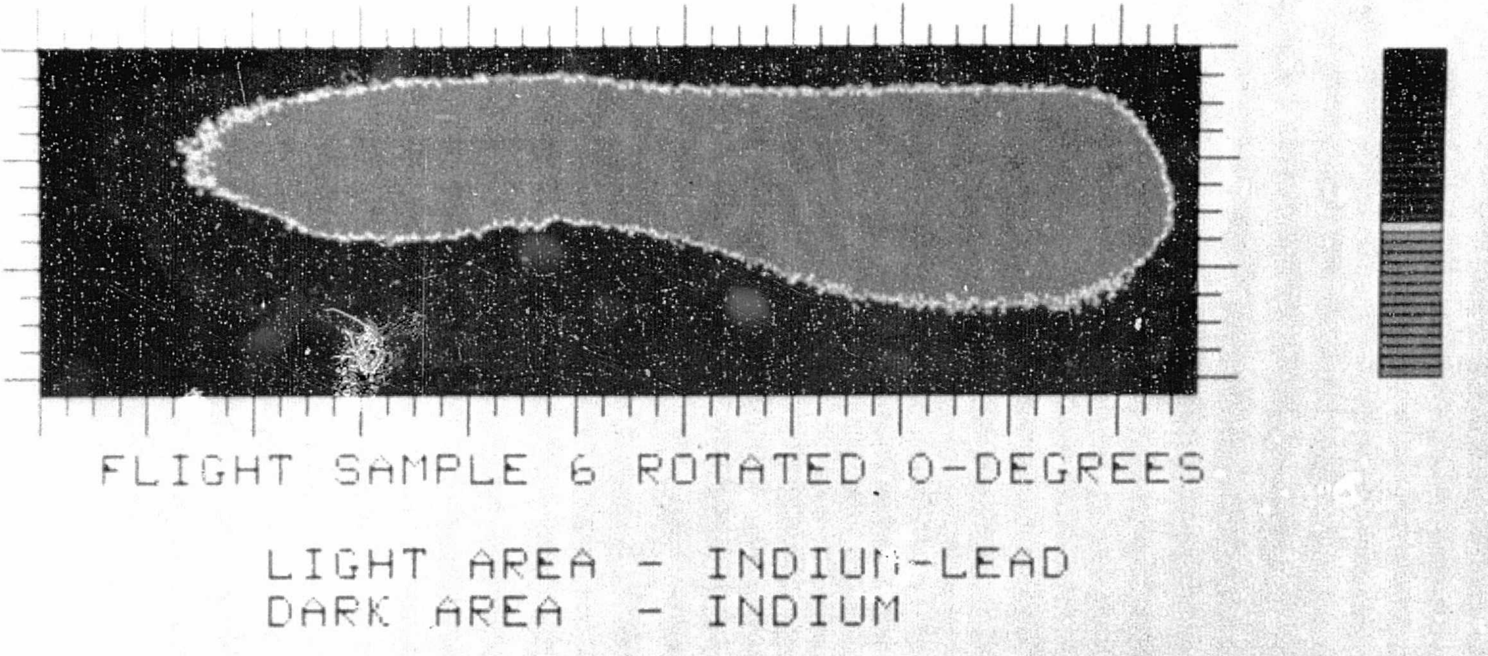

c. Pseudocolored: same scheme as used in Figure 3b.

Figure 4. (Concluded).

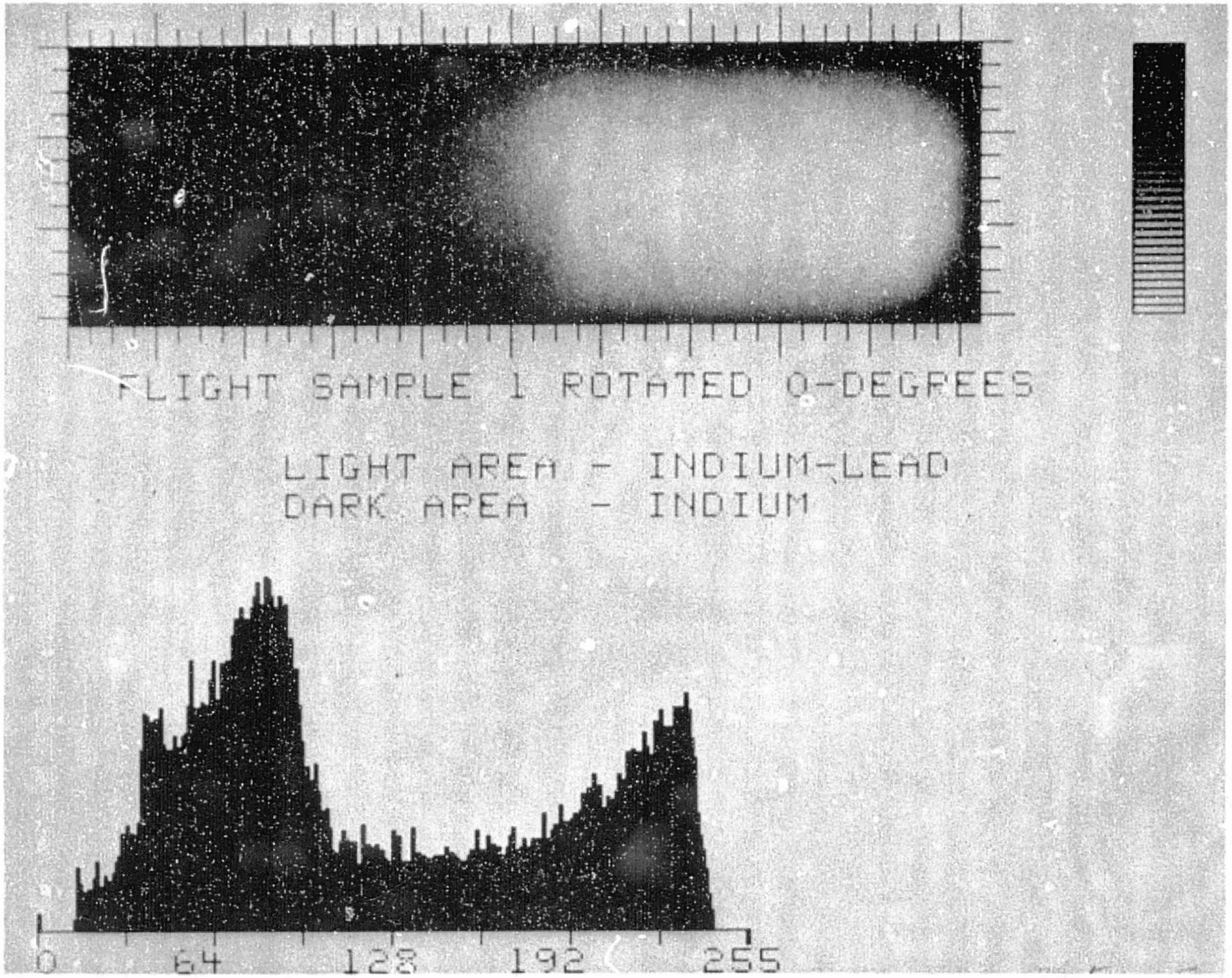

a. Edge enhanced.

Figure 5. Entire image of sample No. 1.

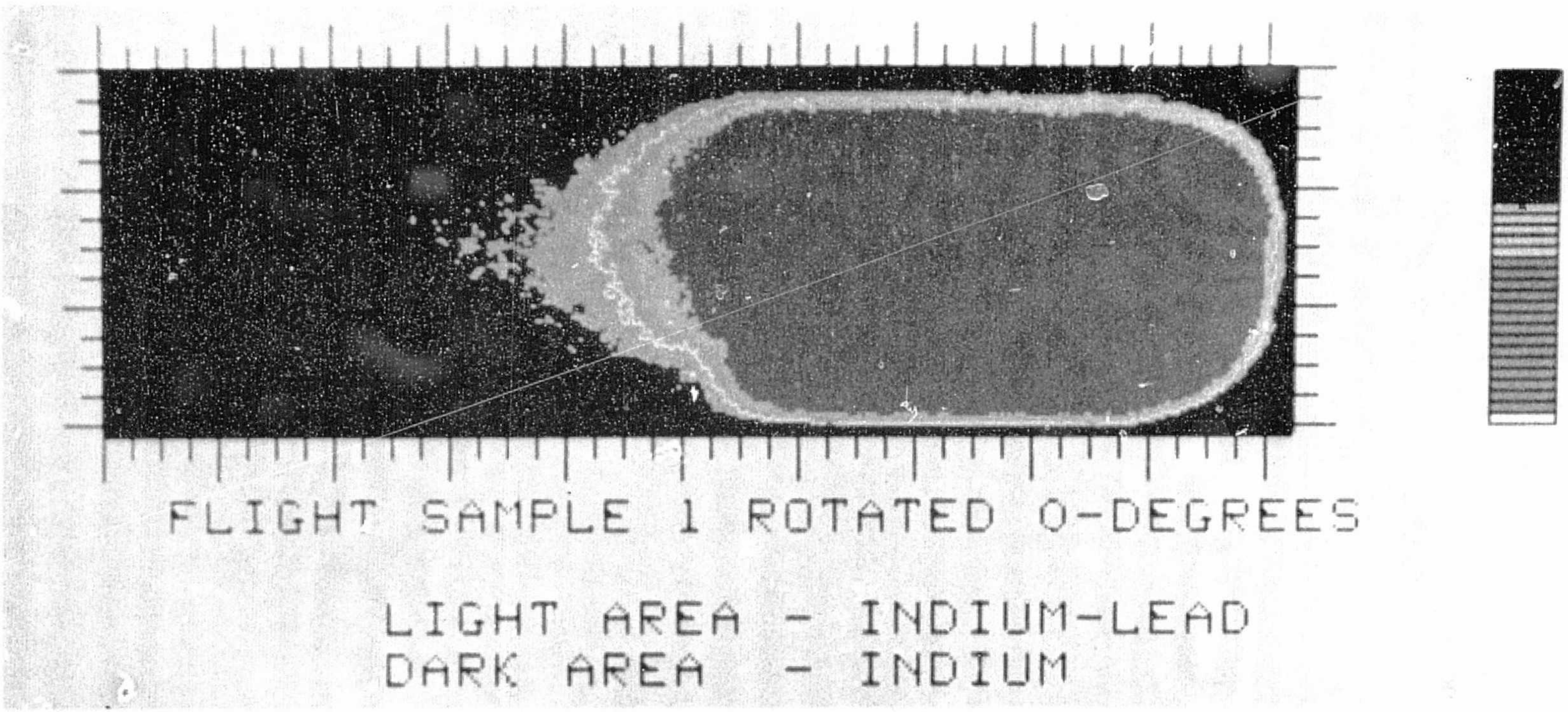

b. Pseudocolored: same scheme as used in Figure 3b.

Figure 5. (Concluded).

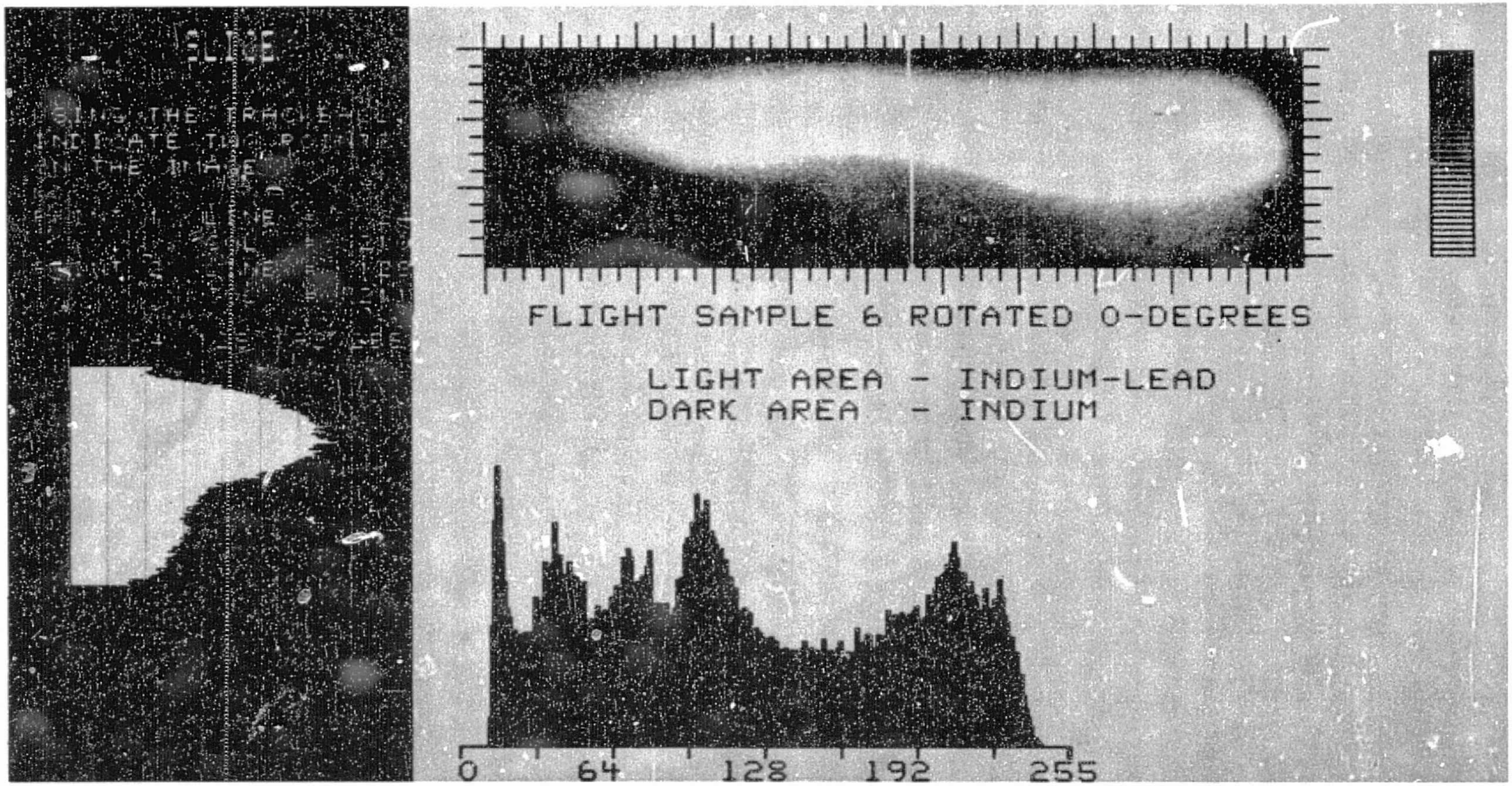

Figure 6. Low-resolution video facsimile copy of the slice operation.

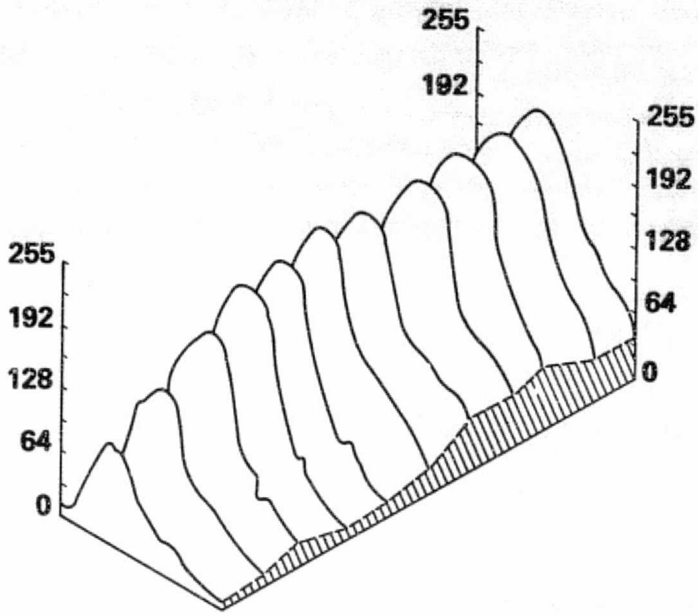

Figure 7. Composite made from slicing operation performed perpendicular to the longitudinal axis of Figure 4a (axis numbers refer to GSV's).

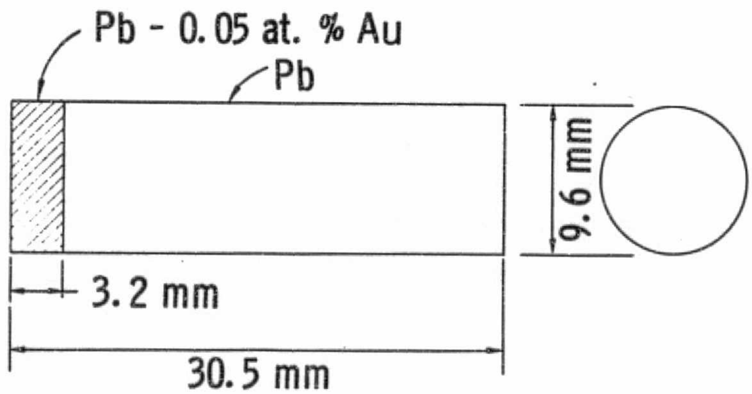

Figure 8. Sample configuration for ASTP Experiment MA-041.

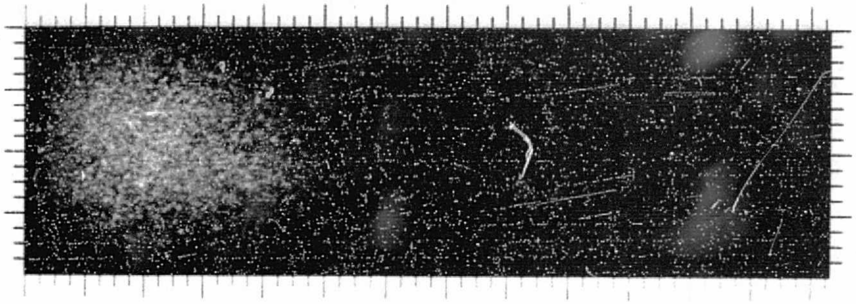

SF 11A 650 DEG. C

MELTING DIRECTION --->

Figure 9. Image converted from GSV's to gold concentration values.

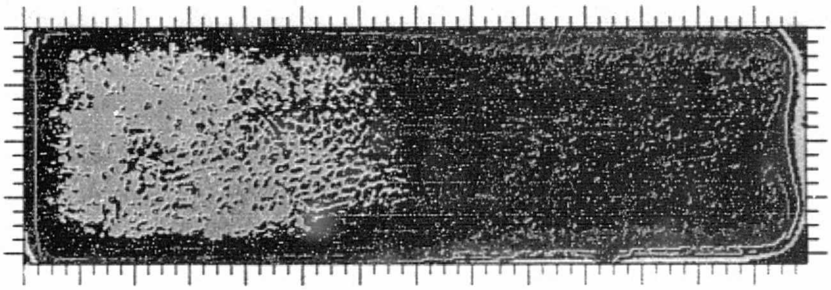

GB 17A 650 DEG. C

<--- MELTING DIRECTION

a. GB sample.

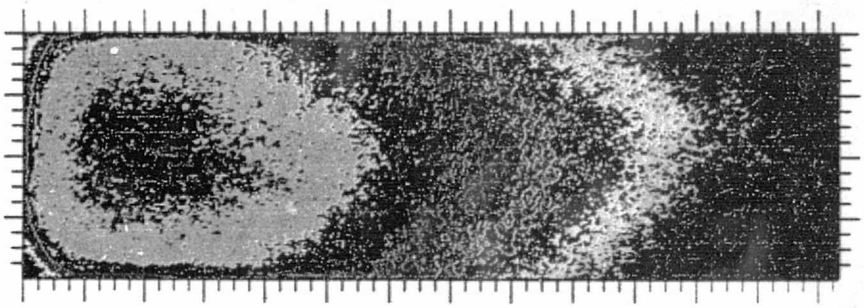

SF 11A 650 DEG. C

MELTING DIRECTION --->

b. Corresponding SF sample.

Figure 10. Pseudocolored GB sample and its corresponding SF sample.

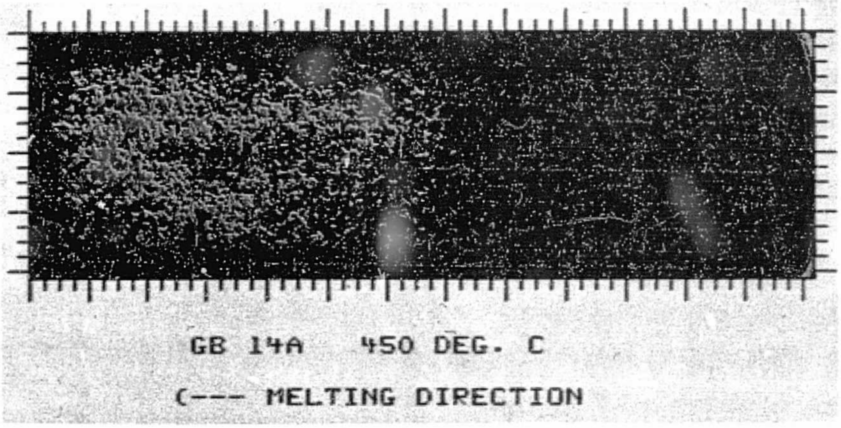

a. GB sample.

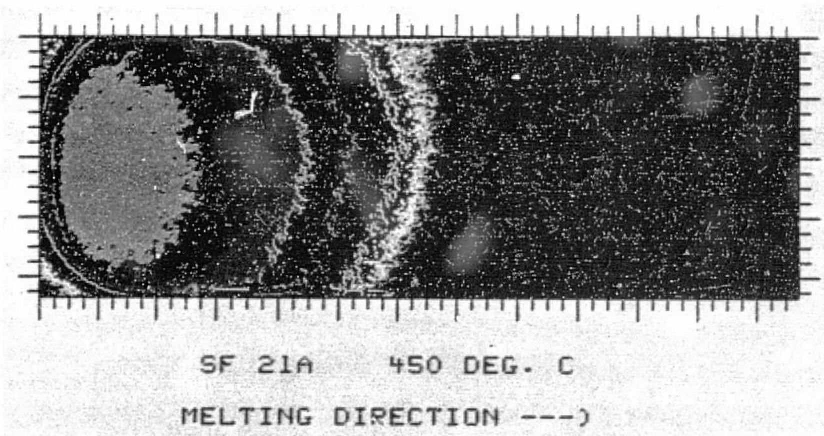

b. Corresponding SF sample.

Figure 11. Pseudocolored GB sample and its corresponding SF sample.

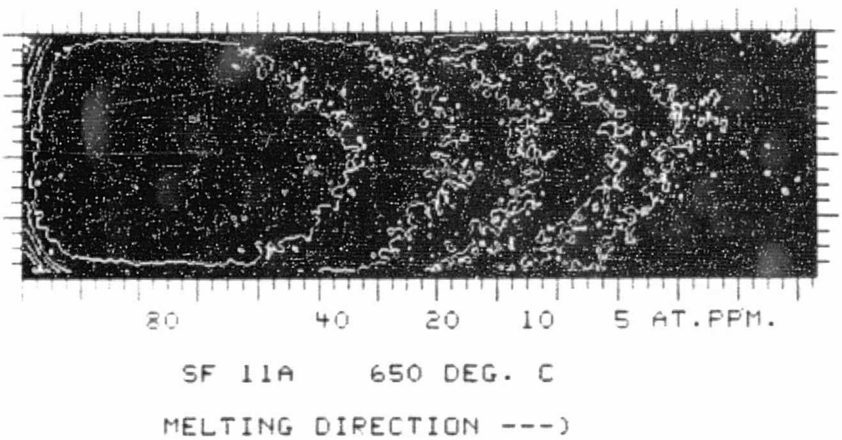

Figure 12. Isogrammed image showing gold concentrations in at. ppm contours as labeled.

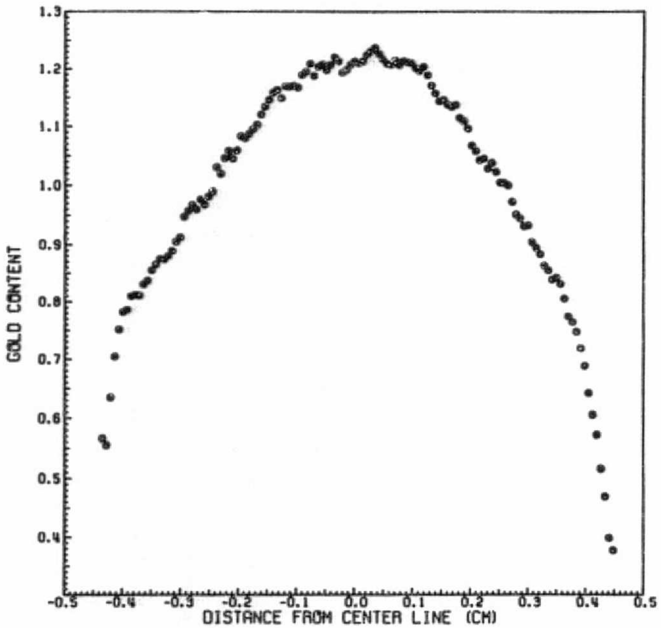

a. The ordinate represents percent of total gold for each slice compared to the initial concentration (500 at. ppm). The abscissa represents the radial location of each slice on either side of the central longitudinal slice (flight sample 11A).

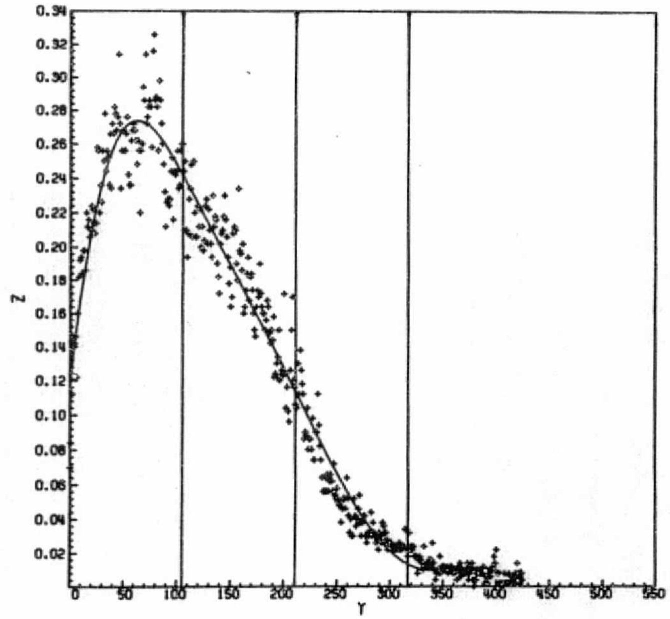

b. The ordinate is same as that of Figure 13a. The abscissa corresponds to a particular column number (in the $N \times N$ image array) which can be easily converted to units of length (central longitudinal concentration slice for flight sample 11A).

Figure 13. Plots of slicing operation.

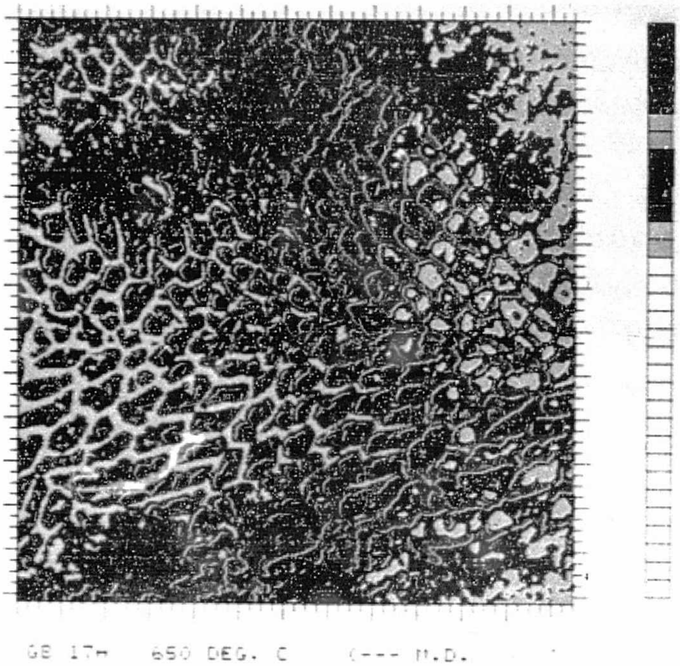

a. GB sample.

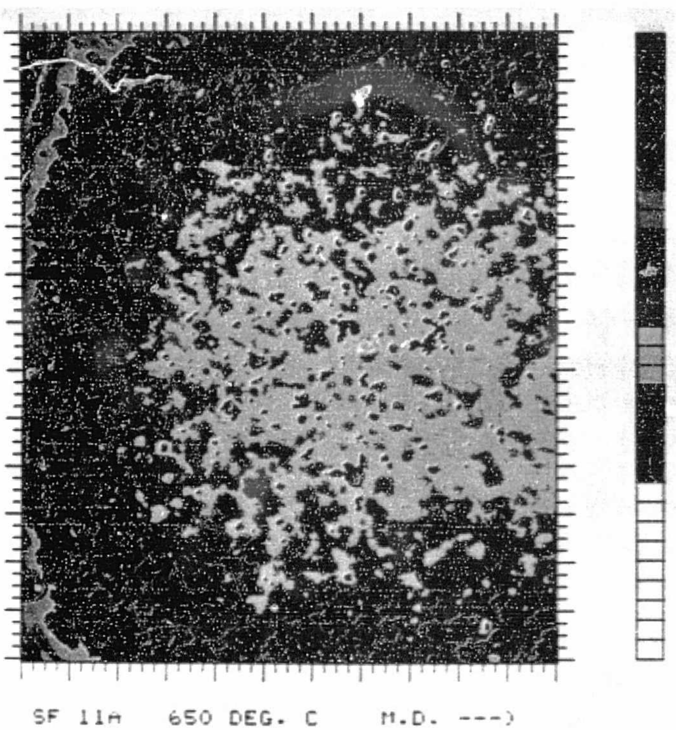

b. Corresponding SF sample.

Figure 14. Microstructure and gold distribution as seen in the GB sample and in the corresponding SF sample.

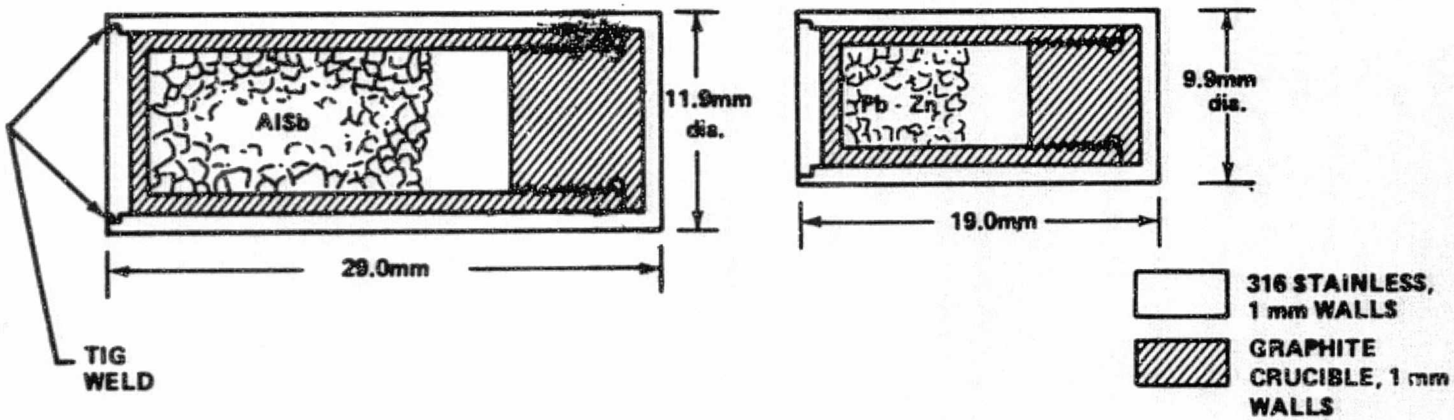

Figure 15. Configuration of AlSb sample (left) and PbZn sample (right) for ASTP Experiment MA-044.

(A185)

a. Low-gravity environment.

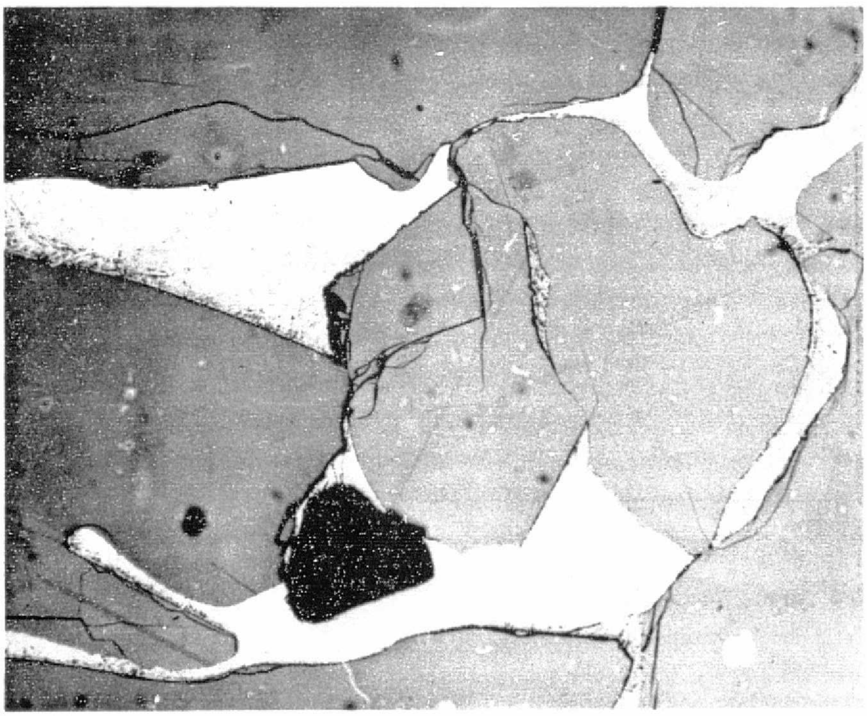

(A141)

b. One-gravity environment.

Figure 16. Comparison of photomicrographs of AlSb.

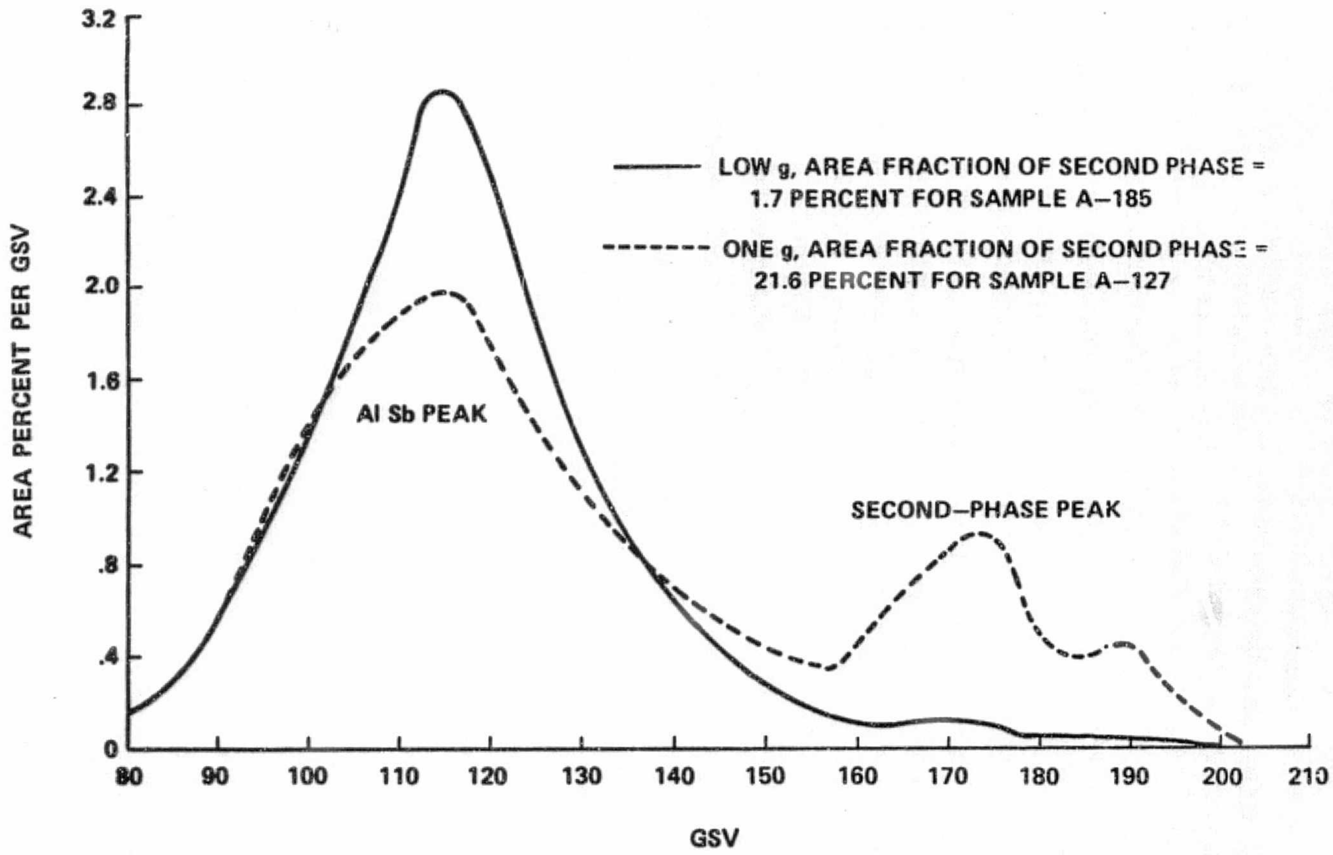

Figure 17. Quantitative comparison of AlSb microstructure using IDAPS histogram operator.

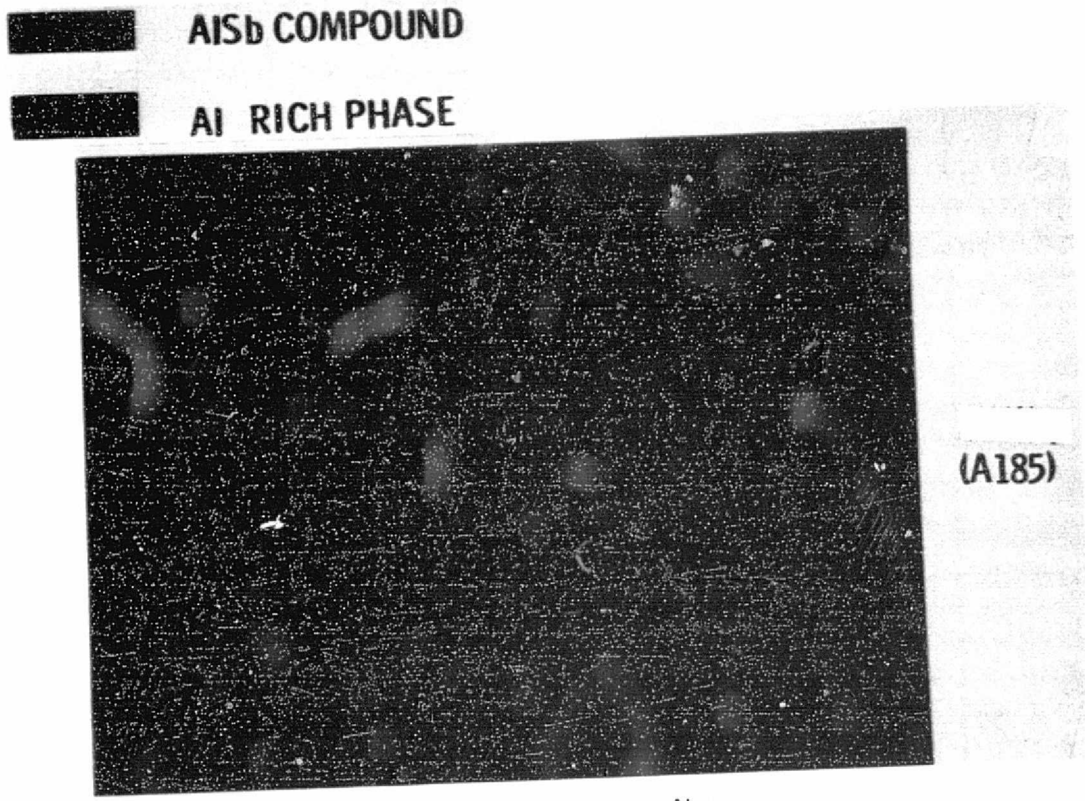

a. Low-gravity.

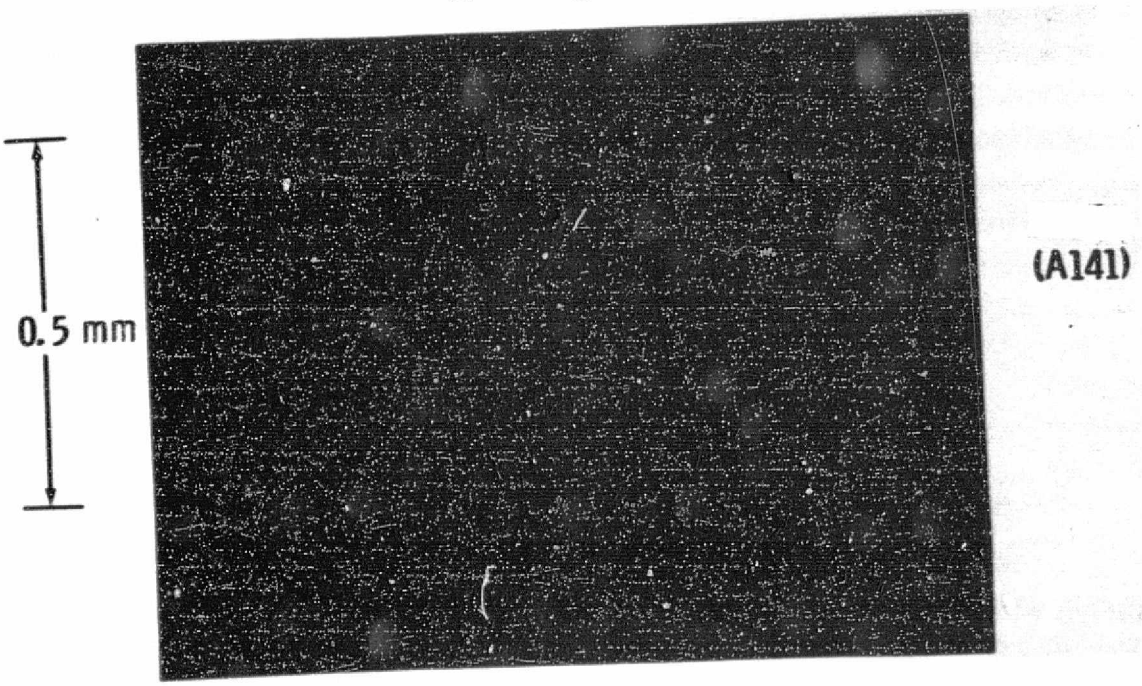

b. One-gravity.

Figure 18. Pseudocolor of photomicrographs of Figure 16.

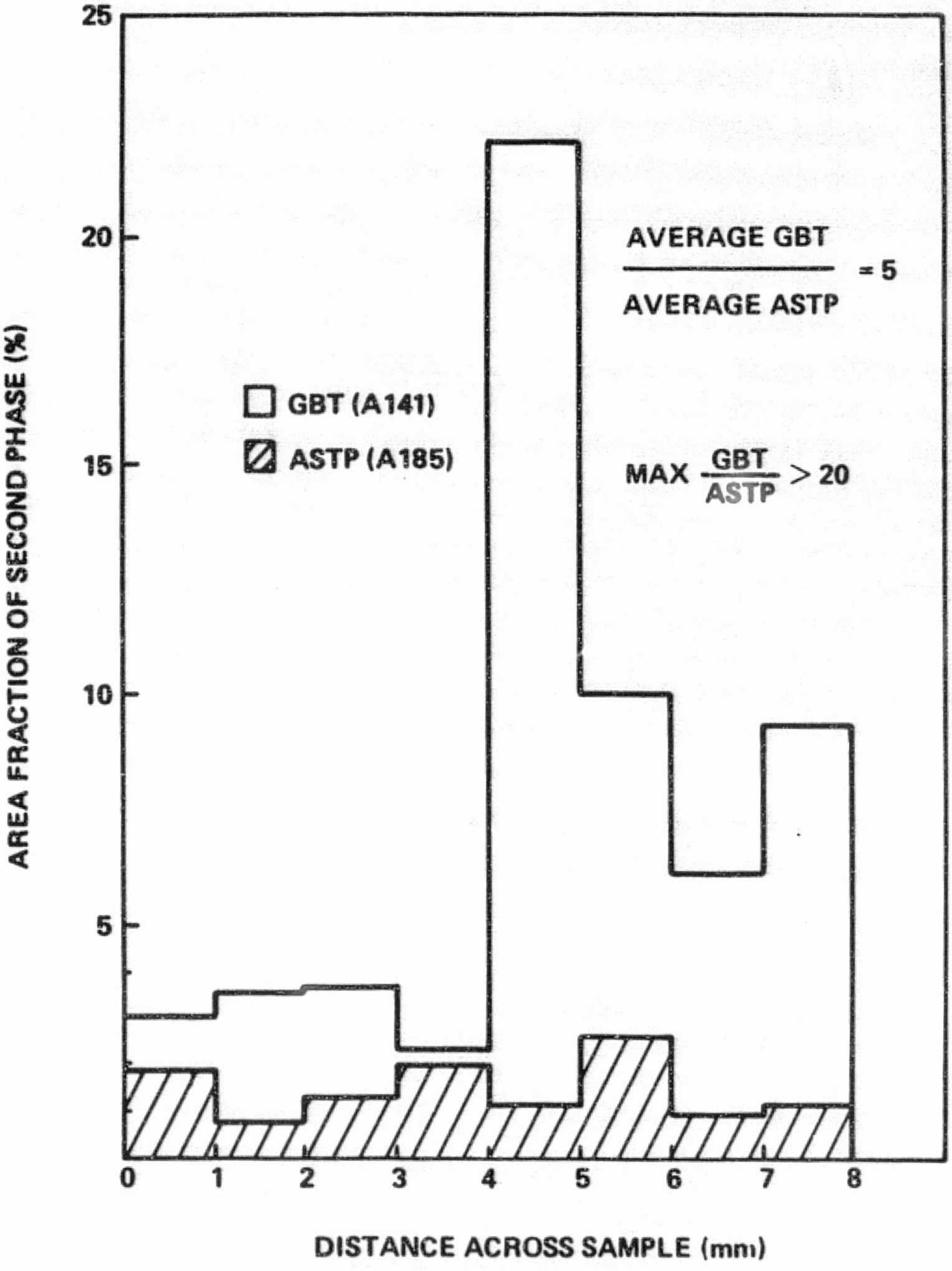

Figure 19. Quantitative histogram data on microstructure of AlSb across sample section.

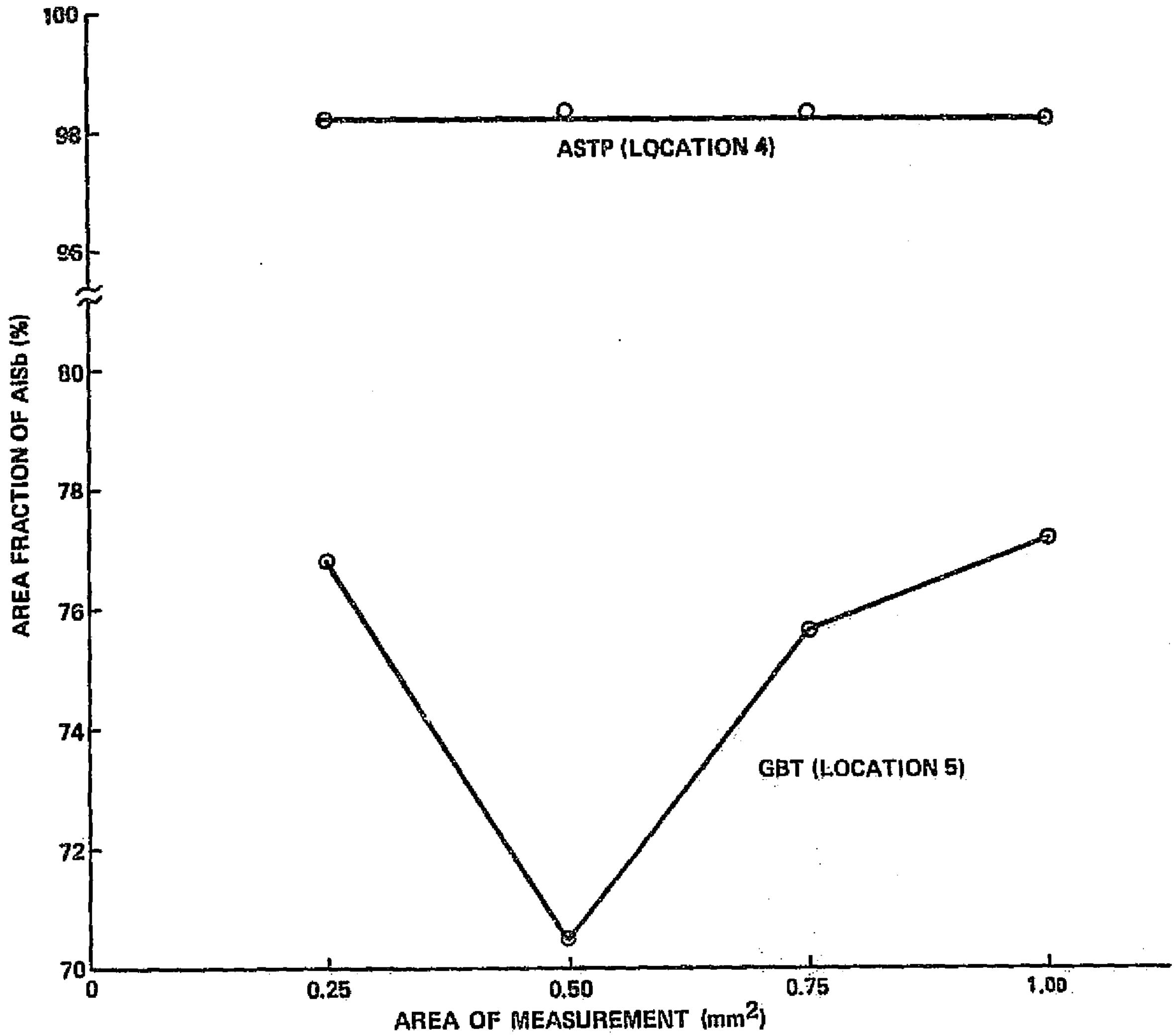

Figure 20. Quantitative histogram data of AlSb homogeneity as a function of microphotographed area.

TABLE 1. IDAPS OPERATORS (IBM 360 AVAILABILITY)

ALTER (Table Lookup)	ROTATE (Large or Small Angles)
AUTOMATIC SCALE (Linear/Nonlinear)	STONYHURST GRID (Spherical Coordinate Plot)
AVERAGE (Multiple Images)	TRANSPOSE (Picture Matrix Operations)
CENTER DIAMETER (Solar Parameter Determination)	MAGNIFY (Expand/Shrink Image)
EXTRACT SUBFRAME	CONVOLUTION FILTER (Filter Weight Convolver)
FRAME (Annotated Display Mask)	DEPENDENT ALTER (Vignetting Correction)
H-D CORRECTION (Film Curve Correction)	SIMILARITY (Window/Picture Cross-Correlation)
INSERT FRAME	DISTANCE (Sun Referenced)
INVERT (Gray Scale Reversal)	FEATURE ANALYSIS (Subset Statistics)
ISOGRAM (Constant Value Contours)	FILTER GENERATOR (Space or Fourier Domain)
LABEL (Annotation Overlay)	FFT (2-D Transform)
MATH (Common Arithmetic Operations)	IFFT (2-D Inverse Transform)
OVERLAY (Controlled Image Superposition)	FOURIER FILTER (Fourier Convolution)
DIFFERENCE PICTURE (Biframe Change Detection)	MASK (Extract/Insert Irregular Subframes)
REGISTER (Biframe Coregistration)	IMAGE MAKER (Test Patterns)

TABLE 2. IDAPS SPECIAL FUNCTION OPERATORS (MINICOMPUTER AVAILABILITY)

Operations Functions:	HELP (Explanatory Messages)
	RETURN TO MASTER MENU (Terminates Terminal Minicomputer Operation; Displays Master Menu)
	SPECIAL FUNCTION EXIT (Terminates Special Function Operation)
Processing Functions:	COORDINATES (Displays Location and GSV around Selected Point on Picture)
	HISTOGRAM (Histogram of Frequency of GSV Occurrence in Selected Rectangle on Picture)
	SLICE (GSV versus Position along a Line)
	QUICK LOOK SCAN (Low-Resolution Scan)
	RESTORE (Transfers Monitor Display to Disk)
	ERASE (Erases Monitor Display)
	GRAY-SCALE WEDGE (Writes GSV Wedge on Picture)
	REPEAT (Multiple Entries)

TABLE 3. COLOR SCHEME RELATING PSEUDOCOLORS TO GOLD CONCENTRATIONS

Pseudocolor	Gold Concentration (at. ppm)	Percentage of Original Gold Concentration
Black	0- 5	0 - 1.0
Yellow	6- 10	1.2- 2.0
Blue-Green	11- 20	2.2- 4.0
Red	21- 40	4.2- 8.0
Green	41- 80	8.2-16.0
Purple	81-120	16.2-24.0
Dark Blue	121-160	24.2-32.0
Orange	161-254	32.2-50.8

REFERENCES

1. Hunt, B. R.: Digital Image Processing. Proc. IEEE, vol. 63, no. 4, April 1975, pp. 693-708.

2. Jesse, A.: Quantitative Image Analysis in Microscopy — A Review. Microscope, vol. 13, January 1971, pp. 21-30.

3. Billingsley, F. C.: Applications of Digital Image Processing. Applied Optics, vol. 9, no. 2, February 1970, pp. 289-299.

4. Wilson, R. M.; Teuber, D. L.; Watkins, J. R.; Thomas, D. T.; and Cooper, C. M.: A Unique Image Data Processing System for Solar Astronomy. Applied Optics, vol. 16, April 1977 (in press).

5. Wray, J. D. and Benedict, G. F.: Some Astronomical Applications for Precision High Speed Computer Interfaced Microdensitometry. Proc. Soc. of Photo-Optical Instru. Eng.: Instrumentation in Astronomy-II, vol. 44, March 1974, pp. 137-146.

6. Richter, P. H.: Enhancement of Ground Based Astronomical Photographs by Digital Image Processing. Proc. Soc. of Photo-Optical Instru. Eng.: Instrumentation in Astronomy-II, vol. 44, March 1974, pp. 215-221.

7. Kruger, R. P.; Andrews, H. C.; and Tescher, A. G.: Image Processing by Digital Computers. IEEE Spectrum, vol. 9, no. 7, July 1972, pp. 20-32.

8. Kruger, R. P.; Hall, E. L.; Dwyer III, S. J.; Hall, D. L.; McLaren, R. W.; and Lodwick, G. S.: A Survey of Preprocessing and Feature Extraction Techniques for Radiographic Images. IEEE Trans. on Computers, vol. C-20, no. 9, September 1971, pp. 1032-1044.

9. Hunt, B. R.; Janney, D. H.; and Zeigler, R. K.: Radiographic Image Enhancement by Digital Computers. Materials Evaluation, vol. 31, no. 1, January 1973, pp. 1-5.

10. Hartmann, F.: X-Ray Mapping of Flaws by Computer Graphics. Materials Evaluation, vol. 27, no. [illegible], August 1969, pp. 169-179.

REFERENCES (Continued)

11. Ekstrom, M. P.: Digital Image Processing at Lawrence Livermore Laboratory, Part I — Diagnostic Radiography Applications. Computers, vol. 7, no. 5, May 1974, pp. 72-80.

12. Nazare, S. and Ondracek, G.: Polarized Light and Dark Field Illumination in Quantitative Structure Analysis. Prakt. Metallogr, vol. 6, 1969, pp. 742-746.

13. Ratz, G. A.: The Niche for Automated Quantitative Microscopy. Metals Progress, 1968, pp. 153-156.

14. Image Data Processing System (IDAPS) User Manual. System Development Corporation Report TM-HU-037/000/00 (1975) (for NASA Contract No. NAS8-30740).

15. Holloway, J. A. and Shelton, W. L.: A Survey of Image Processing Methods for Radiography. Materials on the Move. Proc. 6th Nat. Tech. Conf., Soc. Adv. Mat. Proc. Eng., October 1974, pp. 110-117.

16. Moore, G. A.: Survey of Factors Controlling the Design of Automatic Systems for the Quantitative Analysis of Micrographs. National Bureau of Standards Report No. 8073, June 1963.

17. Wilson, R. M.; Teuber, D. L.; Watkins, J. R.; Thomas, D. T.; and Cooper, C. M.: The MSFC Image Data Processing System — IDAPS. Submitted to IEEE Computer Magazine, 1976 (preprint available from author).

18. Schafer, C. F. and Rathz, T. J.: Experiment 74-18, Liquid Mixing Experiment. Space Processing Applications Rocket Project — SPAR I Final Report, NASA TM X-3458, 1976.

19. Schafer, C. F. and Fichtl, G. H.: SPAR I Liquid Mixing Experiment. AIAA Paper No. 77-119, AIAA 15th Aerospace Sciences Conference, Los Angeles, California, January 1977.

REFERENCES (Concluded)

20. Reed, R. E.: Surface-Tension-Induced Convection — Experiment MA-041. Apollo-Soyuz Test Project: Preliminary Science Report, NASA TM X-58173, February 1976.

21. Reed, R. E.; Uelhoff, W. and Adair, H. L.: Surface Tension Induced Convection in Encapsulated Liquid Metals in a Microgravity Environment. ASTP Experiment MA-041 Final Report, Oak Ridge National Laboratory Report No. 5241, November 1976.

22. Ang, C. Y. and Lacy, L. L.: Low-Gravity Homogenization and Solidification of Aluminum Antimonide. Progress in Astronautics and Aeronautics: Material Sciences with Applications to Space Processing, vol. 49, Leo Steg (ed.), American Institute of Aeronautics and Astronautics, 1976.

23. Lacy, L. L. and Ang, C. Y.: Monotectic and Syntectic Alloys, Experiment MA-044. Apollo-Soyuz Test Project: Preliminary Science Report, NASA TM X-58173, February 1976.

APPROVAL

THE APPLICATION OF DIGITAL TECHNIQUES TO THE ANALYSIS OF METALLURGICAL EXPERIMENTS

By Thomas J. Rathz

The information in this report has been reviewed for security classification. Review of any information concerning Department of Defense or Atomic Energy Commission programs has been made by the MSFC Security Classification Officer. This report, in its entirety, has been determined to be unclassified.

This document has also been reviewed and approved for technical accuracy.

JOHN R. WILLIAMS
Acting Chief, Solid State Branch

ROBERT J. NAUMANN
Chief, Space Processing Division

CHARLES A. LUNDQUIST
Director, Space Sciences Laboratory